Journal of Building Engineering 104 (2025) 112210

Contents lists available at ScienceDirect

Journal of Building Engineering

journal homepage: www.elsevier.com/locate/jobe

Jute fiber reinforcement for masonry walls: Integrating structural strength and thermal insulation in sustainable upgrades

Flavio Stochino [a,*], Arnas Majumder [a], Andrea Frattolillo [a], Monica Valdes [a], Enzo Martinelli [b]

[a] Department of Civil Environmental Engineering and Architecture, University of Cagliari, via Marengo 2, 09123, Cagliari, (CA), Italy
[b] Department of Civil Engineering, University of Salerno, via Giovanni Paolo II n.132, 84084, Fisciano, (SA), Italy

A B S T R A C T

Existing masonry buildings require appropriate structural and thermal upgrading to meet structural safety and energy efficiency according to the current standards. Textile Reinforced Mortar (TRM) presents several advantages for masonry strengthening, but the production of man-made fibers is often expensive and environmentally harmful. For this reason, this work reports on the integrated (structural and thermal) upgrading of the hollow-clay brick masonry walls strengthened with jute Natural Fiber (NF) TRM system configured with jute fiber nets, jute fiber diatons and jute fiber composite mortar. The shear strength capacity and ultimate strength of these upgraded masonry walls have been evaluated through in-plane cyclic shear tests, whereas a constant vertical load was applied. Furthermore, the thermal performance of the same upgraded masonry walls has been evaluated through thermal conductance measurement, by using a climate chamber with pre-set environmental (internal/room and external/ambient) conditions.

Masonry wall specimens were upgraded with NFTRM system package and the package consists of fiber nets (with mesh 2.5 cm × 2.5 cm, one on each side), jute fiber diatons (four), and jute fiber composite mortar (of the combination of 1 % jute fiber with respect to the dry mortar mass and 30 mm fiber length).

Improvements in both ultimate strength and thermal insulation of the NFTRM-upgraded masonry walls have been observed as part of the integrated (structural and thermal) behavior assessment.

Due to the application of jute fiber composite layers of the NFTRM system package (jute fiber nets, jute fiber diatons, and jute fiber composite mortar) the overall withstanding load capacity increased by more than 525.00 %, whereas the thermal transmittance value was reduced by 36.05 % (representing the improvement of insulation capacity) when compared with the masonry wall without upgrading.

1. Introduction

About 85% of buildings in the European Union (EU) were constructed before 2001 [1] and most of them are masonry buildings [2]. These buildings have predominantly been designed and constructed considering only vertical loads [3] without respecting any seismic safety [4] and energy-efficiency standards. In addition, part of these buildings present also an important cultural value, and its safety and retrofitting require particular attention [5–7]. A significant portion of EU buildings is vulnerable to seismic risks [8], and nearly 75 % of them are also energy inefficient [9]. As reported by IEA (2022), the global final energy consumption and total CO_2 emissions due to building operations in the year 2021 were found to be around 30 % and 27 % i.e., respectively equal to 135 GJ and 10 $GtCO_2$ [10]. These buildings urgently need upgrading to meet the latest seismic standard [11] as well as to achieve the thermal performance goal [12], required by EU directives [13]. It is interesting to underline that the amended energy performance and buildings directive of

* Corresponding author.
E-mail addresses: fstochino@unica.it (F. Stochino), arnas.majumder@unica.it (A. Majumder), andrea.frattolillo@unica.it (A. Frattolillo), m.valdes@unica.it (M. Valdes), e.martinelli@unisa.it (E. Martinelli).

https://doi.org/10.1016/j.jobe.2025.112210
Received 31 October 2024; Received in revised form 17 February 2025; Accepted 23 February 2025
Available online 25 February 2025

2018 [13] encourages to implement the measures for fire safety and seismic risk strategy, also promoting thermal-structural upgrade or retrofitting.

In the real Construction and Building (C&B) field, organic, inorganic, and mineral fibers (like carbon, basalt, steel, Polypropylene, etc.) are used for structural retrofitting purposes.

Textile Reinforced Mortar (TRM) systems are particularly suitable for upgrading and/or retrofitting masonry structures, due to their high strength-to-weight ratio enhancing the overall mechanical performance and it has lower stress concentration due to higher homogeneity between TRM and masonry [14]. Moreover, there is better chemical and physical compatibility between composite and masonry substrates [15] and good performance even after fire exposure [16]. However, no dedicated standards are currently available to design, test, and/or qualify the TRM system [15,17], other than, the standard and guidelines RILEM TC 250-CSM (2016) [18] and ACI 549.4R-13 (2013) [19] developed by the United States (US). More recently another guideline CNR-DT (2018) [14] has been prepared by the Italian National Research Council.

Notably, manmade (organic and inorganic) and mineral fabric/textile/net [20] are available commercially for TRM retrofitting, and some interesting experimental applications in the construction and building sector can be highlighted as carbon-TRM [21–25], glass-TRM [26–29], basalt-TRM [30–32], steel-TRM [33,34] and polypropylene-TRM [26,28] systems, respectively. An analytical model for in-plane resistance of masonry walls upgraded with steel fiber-reinforced mortar has been proposed by Ref. [35].

Actually, jute fiber is the second most produced natural plant fiber with many applications like waste jute fiber panels [36], jute/epoxy composites [37], jute-lime composite mortar [38], jute-mortar composite [39–42], jute-clay insulation block [43], jute fiber-reinforced concrete [44], jute fiber reinforced compressed earth bricks [45], etc. Recently Natural Fiber (NF) TRM systems have gained more attention in the construction sector. Menna et al. [46] have strengthened eight masonry panels (walls) made of Neapolitan yellow tuff bricks and solid clay bricks using the hemp-TRM system (consisting of hemp fiber-net and pozzolanic and lime-based mortars) and conducted the diagonal compression test to measure the increment in maximum shear strength of the reinforced masonry panels. Ferrara et al. [15] have developed a flax-TRM system (consisting of flex fibers and hydraulic lime mortar) to strengthen the masonry walls made of clay bricks. Later these walls were subjected to the diagonal compression test. Two different TRM systems were used for strengthening purposes, the first type has one layer of fabric and mortar, while the other type has two layers of fabric and mortar. In this case, too, the authors have stated to have noticed an increment in shear capacity by 118 % and 136 % for the first and second types, respectively. Trochoutsou et al. [47] have studied the mechanical behaviors of the flex-TRM and jute-TRM systems showcasing the potential of the jute fiber-based NFTRM system for structural applications.

Integrated thermal and structural upgrading plays a pivotal role in enhancing the sustainability and resilience of existing buildings. By synergizing thermal improvements with structural enhancements, we not only optimize energy efficiency but also bolster the overall durability of the structure. This integrated approach ensures a harmonious balance, addressing both environmental concerns and structural integrity. Moreover, it contributes to prolonged building lifespan, reducing maintenance costs and minimizing the environmental footprint associated with frequent renovations. In the last years, many researchers have focused on this theme. Thermal and seismic upgrading of existing walls have been obtained using prefabricated textile-reinforced concrete panels [48]. Structural and thermal retrofitting of a masonry wall structure have been investigated in Triantafillou, T.C. et al. (2017) [49] considering a commercially available fabric-TRM system and Expanded Polystyrene (EPS) for this purpose. Further, Triantafillou, T.C. et al. (2018) [50] has used glass-TRM and EPS for structural and thermal retrofitting, respectively. The structure performance of the retrofitted masonry walls in Refs. [49,50] was evaluated through out-of-plane tests and in-plane tests, respectively. Whereas Gkournelos, P.D. et al. (2020) [51] have assessed the Glass-TRM retrofitted masonry wall strength through both out-of-plane tests and in-plane tests, respectively. They have also used EPS for masonry wall thermal upgrading. Karlos, K. et al. (2020) [52] has provided detailed analytical, numerical, and out-of-plane experimental data for glass-TRM retrofitted walls, in this case, EPS has been used for thermal insulation capacity. In Facconi, L. et al. (2021) [53], the structural (with steel-TRM) and thermal (aerogel, light, and heavy wood fiber) properties were evaluated using experimental and numerical models. Interestingly in Longo, F. et al. (2021) [54], the experimental data related to both structural (steel-TRM, glass-TRM) and thermal (natural hydraulic lime and Geopolymer lime) retrofitting are provided, while in Ref. [54] it has been reported to have achieved higher ductility and improved thermal insulation capacity for the Geopolymer-based TRM system. Baek, E. et al. (2022) [55] have proposed an interesting thermo-structural retrofitting technique. They have used Basalt-TRM for structural upgrading, whereas an innovative Textile capillary tube panel (TCP) layer has been used to Improve the insulation property of the masonry wall. Authors have reported to have used hot water to channel it through the tube to obtain the desired room temperature. Again Gkournelos, P.D. et al. (2023) [56] have studied the in-plane and out-of-plane behaviors of the masonry wall retrofitted with commercially available man-made fiber TRM and EPS system and experimental findings were compared with the numerical results. Furtado, A. et al. (2023) [57] used Glass-TRM, External Thermal Insulation Composite System (ETICS) and Reinforced Insulation Mortar (RTIM) in different combination for integrated (structural and thermal) retrofitting. Authors have provided experimental data on the out of plane structural tests, while the thermal transmittance values have been calculate based on the thermal conductivity values of the used materials. In aforementioned research [49,50,51,52,56], authors have considered without conducting any experiment that the EPS has induced improvement, in the thermal insulation capacity of the wall.

As far as it is known, there are no studies, research works, or data available on the integrated (structural and thermal) retrofitting or upgrading properties of a NFTRM system, or more specifically on the jute fiber products NFTRM system, with direct application on the real scale for masonry walls. In order to bridge this gap, this paper provides a comprehensive study on the structural properties and thermal behaviors of the upgraded masonry walls strengthened with jute fiber products (jute nets, jute fiber diatons, and jute fiber composite mortar).

The structural and thermal strengthening parameters were evaluated through the in-plane cyclic test and thermal conductance test, respectively. This is a follow-up of the previous research activities that can be found in Refs. [2,58,59]. The innovations presented in

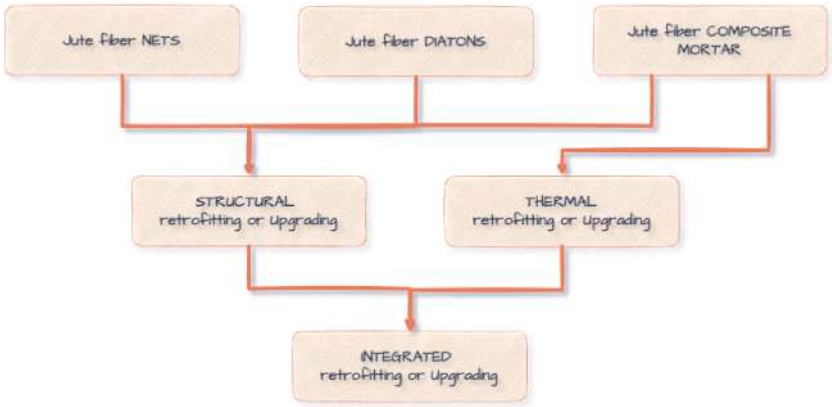

Fig. 1. The use of jute fiber products (nets, diatons and composite mortar) for integrated retrofitting/upgrading.

this work are as follows:

- Natural fiber has been employed for dual purposes – both structural reinforcement and thermal enhancement – seamlessly integrated into a masonry wall/structure using a NFTRM system. The primary objective is the comprehensive investigation of both the structural and thermal properties.
- Various jute fiber products such as nets, diatons, and chopped raw fibers (for composite mortar) have been utilized for the integrated upgrading within the NFTRM system.
- An experimental assessment of the thermal properties has been conducted within a dedicated climate chamber. This involved maintaining specific environmental conditions, encompassing internal room settings and external ambient conditions.
- A complete *TRM system package*, comprising jute fiber nets, jute fiber diatons, and jute fiber composite mortar, has been developed. This holistic approach aims not only to enhance structural behavior but also to elevate the thermal performance of the upgraded masonry wall/structure. It has been nominated as a *TRM system package*, as a unique TRM system was fabricated with the capability to improve both structural and thermal performances. In our case, the thermal insulation is provided by the natural fiber (jute) composite mortar which is an integral part of the TRM system.

This paper is divided into four sections. After this brief introduction, Section 2 presents the various materials used for this experimental campaign, and methods and processes used for conducting tests. Section 3 shows the result and findings from various tests with the corresponding discussions. Some conclusive remarks are drawn in Section 4.

2. Materials and methods

Fig. 1 illustrates the integrated retrofitting or upgrading scheme, showcasing the application of various jute fiber products for this purpose. All the manufacturing and testing activities have been developed in the Material Strength Laboratory (for the structural part) and in the Applied Thermodynamic and Energy Laboratory (for the thermal part) of the University of Cagliari (Italy).

Fig. 2. (a) Raw jute fibers and (b) fiber cutting process.

Fig. 3. Jute fibers cut into (a) 30 mm, (b) 10 mm and (c) 5 mm fiber lengths.

Table 1
Mechanical properties of jute fiber [58].

Tensile strength [MPa]	215.1 (with C.oV. of 4.4 %)
Strain energy [kNmm]	0.8 (with C.oV. of 58.9 %)
Maximum axial stain	0.013 (with C.oV. of 19.1 %)
Young's modulus [GPa]	17.0 (with C.oV. of 17.9 %)

Fig. 4. Jute diatons.

2.1. Raw jute fibers

The raw jute fibers (Fig. 2a) variety is Bangla Tosha - Corchorus olitorius (golden shine). They are harvested in West Bengal, India. During this experimental campaign the fibers (about 3–4 m long) were manually cut (Fig. 2b) into three different sizes 30 mm, 10 mm and 5 mm (Fig. 3). The average diameter of the raw jute fiber specimen found to be about 81 μm [58]. The mechanical properties of the jute fibers are presented in Table 1.

2.2. Jute diatons

Horizontal Connectors (HC) like timber, bamboo, reed and stones have been used traditionally for centuries by various civilizations. HC are sometimes also called as transversal connectors or diatons. It is an important structural element mainly inserted orthogonally into the masonry wall to connect its two external surfaces, with the aim to improve the shear resistance of the applied structures, and also tie the leaves of the wall and prevent their separation.

Notably this is the first research work, in which jute fiber made diatons, see Fig. 4, are used for masonry wall retrofitting/upgrading. Whereas during this research, the choice of using the diatons alone with jute nets for the single-leaf hollow clay brick walls was due following motivation:

(1) Anchoring/connecting the Textile Reinforced Mortar (TRM) net systems applied to two surfaces of the wall.
(2) Provide additional strength NFTRM system (as tested jute fiber net used for this project is relatively less strong than that of man-made fibers carbon, basalt or steel fibers generally are used for TRM retrofitting)
(3) To improve/enhance the masonry walls shear capacity.

Diatons (Fig. 4) are manually fabricated with the same jute fibers and have a diameter about 15.5 mm (9.68 % Co.V.). Authors have already characterized these diatons, and their fabrication process, physical properties and mechanical behaviors are reported in Ref. [58] and in Table 2.

Table 2
Mechanical properties of jute diatons [58].

Tensile strength [MPa]	15.5 (with C.oV. of 20.8 %)
Strain energy [kNmm]	14.18 (with C.oV. of 53.9 %)
Maximum axial stain	0.03 (with C.oV. of 23.6 %)

2.3. Jute net fabrication

Fig. 5a presents the jute threads of class 1 mm (for details see [60]) has been been used to fabricate two types of jute nets manually (Fig. 5b), and with configurations 1 m × 1 m (Fig. 6b) and 0.9 m × 0.7 m (Fig. 6c). Both net types have internal mesh pattern of "2.5 cm × 2.5 cm" (Fig. 6a, b and c). The mechanical properties of the jute nets have been experimentally assessed and here briefly reported: see Fig. 7 and Table 3.

2.4. Structural mortar

A cement-based mortar has been used during this campaign for the masonry walls upgrade. In the following sections it would be referred to as "Structural Mortar" (SM). It is classified as M10 class according to Refs. [61,62]. It is a high-performance premixed masonry mortar designed for thin-layer applications in external structures requiring structural compliance according to UNI EN 998-2 [63]. The premixed powder mortar is specifically designed for bedding blocks and stones, composed of cement and carefully selected aggregates to ensure optimal granulometry and purity. It is supplied as a fine powder with a maximum granulometry of 2.0 mm. With a water content of approximately 18 %, the dry apparent density of the product is 1545 kg/m^3 ± 3 %, while the fresh mortar density reaches 2029 kg/m^3 ± 3 %. Its capillary water absorption is 0.8 kg/(m^2·min$^{0.5}$), and it has an A1 fire resistance rating. The chloride content is limited to 0.05 % Cl, ensuring durability and reduced risk of corrosion for embedded reinforcement. The compressive strength at 28 days conforms to M10 (10 MPa) [63], with an initial shear strength of 0.3 N/mm^2. Additionally, it exhibits a thermal conductivity of 0.83 W/mK.

2.5. Jute fiber composite mortar

The jute fiber composite mortar (Fig. 8 and Table 4) was prepared using 1 % of jute fiber (30 mm) with respect to the dry SM mass. The composite mortar mixture was prepared in accordance with EN 1015-2 [64]. Approximately 22 % of water with respect to the total mass (structural mortar + jute fiber) has been used for composite mortar preparation. During the preparation of the composite samples, the fibers were first blended with the dry mortar for 30 s in the dry state without any water, then the required amount of water was added, and the mixture was thoroughly mixed for approximately 10 min. Notably, the necessary amount of water for the mixture was pre-determined using the water absorption test (for further details, see Ref. [58]). Table 4 presents the composite mortar mixture composition used during this campaign.

2.6. Choice of jute fiber length and fiber percentages

The fiber length (30 mm) and fiber percentage (1% with respect to the dry SM mass) have been selected for this campaign. Notably, mainly two factors have been considered before taking this decision:

(i) A balanced approach (Table 5) has been considered while choosing the fiber length and fiber combination, and it is based on authors' previous research activities [58,59]. Therefore, the goal was to achieve the best thermo-mechanical characteristics through integrated masonry retrofitting/upgrading. Notably, the sample MSF1(30) found to have intermediate values for all thermo-mechanical properties (thermal conductivity, strain energy, flexural strength, and compressive strength), which are considered.

Fig. 5. (a) Jute threads of class 1 mm, and (b) Jute net fabrication.

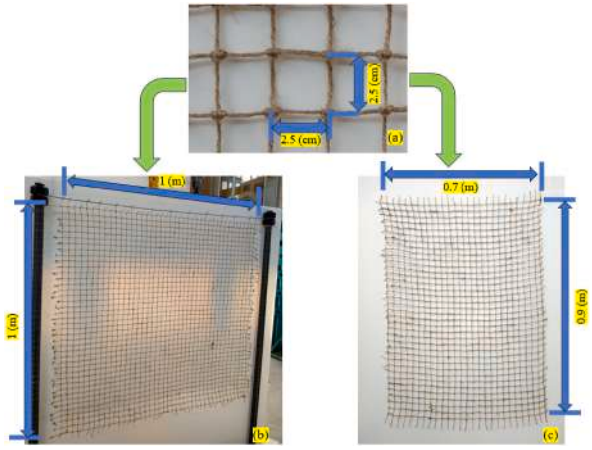

Fig. 6. (a) Jute mesh type: 2.5 cm × 2.5 cm, (b) jute net with a dimension of 1 × 1 m^2 for structural retrofitting/upgrading, and (c) jute net with a dimension of 0.9 × 0.7 m^2 for thermal retrofitting/upgrading.

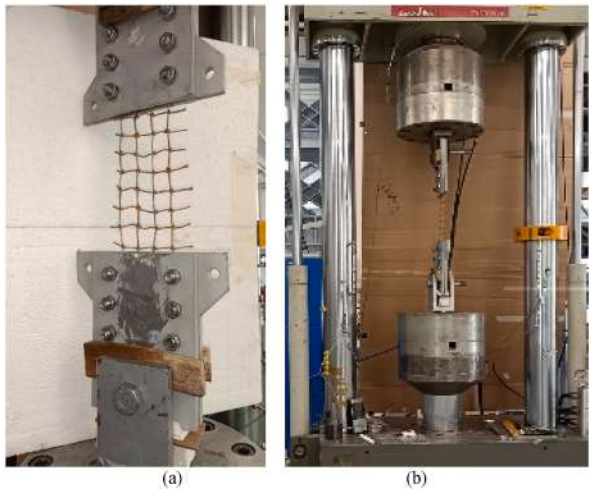

Fig. 7. (a) Net sample 2.5 cm × 2.5 cm placed in the machine for the tensile strength test, and (b) Schenck universal machine used for tensile strength tests.

Table 3
Mechanical properties of jute fiber net of configuration 2.5 cm × 2.5 cm [60].

Stiffness [N/mm]	7.6 (with C.oV. of 20.2 %)
Strain energy [kNmm]	8.8 (with C.oV. of 39.1 %)
Maximum load [N]	217.3 (with C.oV. of 24.8 %)
Maximum displacement [mm]	72.5 (with C.oV. of 17.8 %)

(ii) Percentage of jute fiber, i.e., equal to 1 % (with respect to the dry SM mass) is considered based on [65], which states that the presence of fiber should not be higher than 1 % in an incombustible composite mixture.

2.7. Bricks and masonry wall

The physical-geometric characteristics of semi-solid brick blocks (Fig. 9a) comply with the requirements established by the recent "Technical Standards for Construction" (Ministerial Decree 17/01/2018) [61]. According to Ref. [66] the bricks used for the construction of masonry walls have dimension and apparent specific gravity of 300 mm × 250 mm x 250 mm and 800 ÷ 860 kg/m^3, respectively. These bricks also comply with the additional requirements for masonry materials to be used for seismic design, like: (1) partitions arranged parallel to the plane of the wall continuous and straight (except for the interruptions allowed in correspondence with any gripping holes); and (2) characteristic compressive strength of elements in vertical direction $f_{Bk} \geq 5$ N/mm^2 and orthogonal in

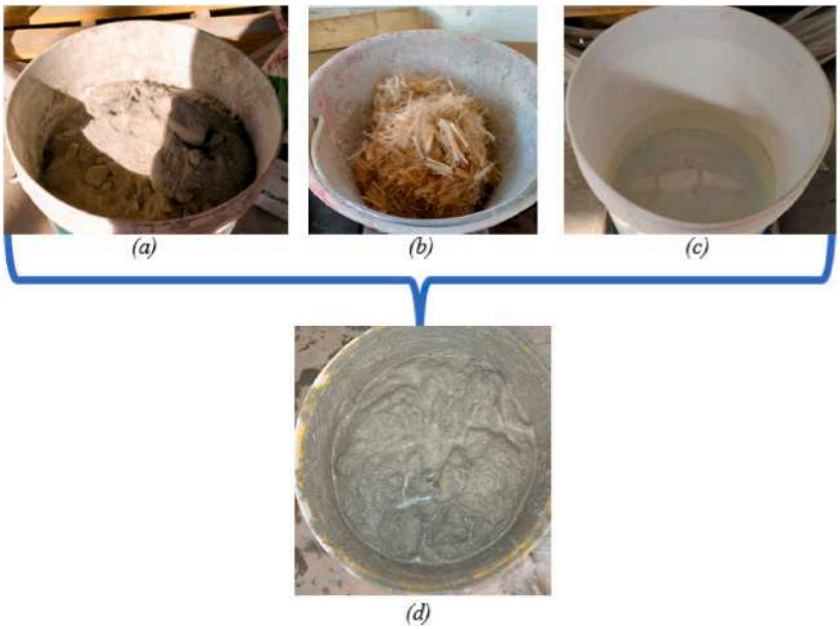

Fig. 8. Composite composition mixture: (a) Structural Mortar (SM), (b) 30 mm jute fiber, and (c) water used, and (d) composite preparation.

Table 4
Jute fiber composite mortar mixture composition, see Ref. [59].

SM	Jute fiber	Water
81.06 %	0.82 %	18.12 %

Table 5
Composite SM mixture combinations used for the masonry wall upgrading (based on results obtained in see Refs. [58,59]*).*

Thermal conductivity at 20°C [W/mK]		
Best value	Intermediate value (selected)	Worst value
MSF1(5) 0.444 (with C.oV of 7.55 %)	MSF1(30) 0.500 (with C.oV of 5.01 %)	MS (No fiber) 0.771 (with C.oV of 3.96 %)
Stain energy [kN.mm]		
Best value	Intermediate value (selected)	Worst value
MSF2(30) 2.687 (with C.oV of 34.84 %)	MSF1(30) 0.551 (with C.oV of 67.01 %)	MS (No fiber) 0.477 (with C.oV of 13.90 %)
Flexural stress [MPa]		
Best value	Intermediate value (selected)	Worst value
MS (No fiber) 7.789 (with C.oV of 8.45 %)	MSF1(30) 5.068 (with C.oV of 7.93 %)	MSF2(5) 3.611 (with C.oV of 10.92 %)
Compressive strength [MPa]		
Best value	Intermediate value (selected)	Worst value
MS (No fiber) 32.25 (with C.oV of 5.61 %)	MSF1(30) 21.83 (with C.oV of 5.79 %)	MSF2(5) 6.03 (with C.oV of 7.47 %)

Note: MS is the structural mortar; F represents the jute fiber, the number after F represents the percentage of jute fiber used in the composite mixture i.e., 1 %, 2 % etc.; (30), (10), and (5) signifies the fiber lengths i.e., 30 mm, 10 mm, and 5 mm, respectively.

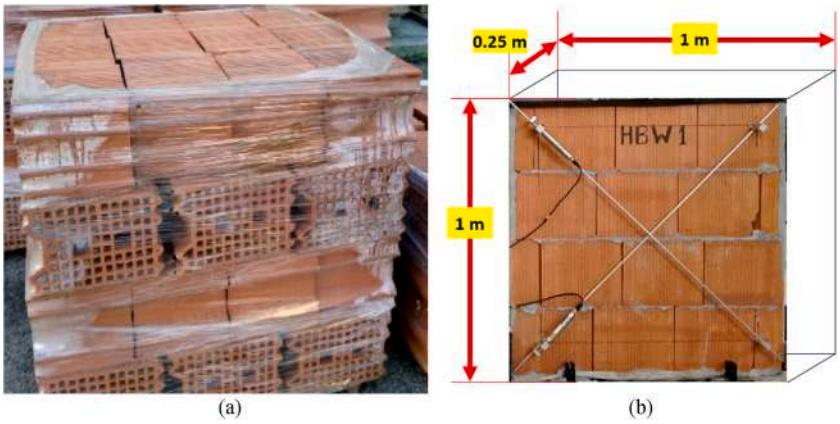

Fig. 9. (a) Hollow bricks, and (b) Hollow Brick Wall (HBW).

the plane of the wall $f'_{Bk} \geq 1.5$ N/mm^2. Fig. 9b shows the dimension of the un-strengthened hollow brick wall.

2.8. Masonry wall construction and test procedure

Two masonry walls have been constructed and tested without any upgrading (HBW1 and HBW2). The masonry walls HBWU (for structural test) HBWU(T) (for thermal test) are reinforced/upgraded with two jute nets (with 2.5 cm x 2.5 mesh configuration), four transversal diatons and jute fiber composite SM (1 % fiber (30 mm) with respect to SM dry mass). This composite retrofitting/upgrading scheme has been labelled as NFTRM system package, see Fig. 10.

Table 6 presents HBWU and HBWU(T) retrofitting schemes. The first layer of SM was applied initially to attach the jute fiber nets on both sides of HBWU and HBWU(T). Thereafter, diatons were inserted through the masonry walls. Afterward, the jute-composite mortar was put on both sides of the masonry.

Wall samples HBWU and HBWU(T) used for structural and thermal tests respectively are similar, and the same NFTRM package configuration with exactly same individual elements (like jute net nets, jute fiber diatons and composite mortar with 1 % (30 mm) jute fiber with respect to the dry mortar mass) has been used for the masonry upgrade. Notably HBWU, the NFTRM strengthened masonry wall has been constructed in one day, while the HBWU(T) wall sample has been constructed step by step to determine the thermal

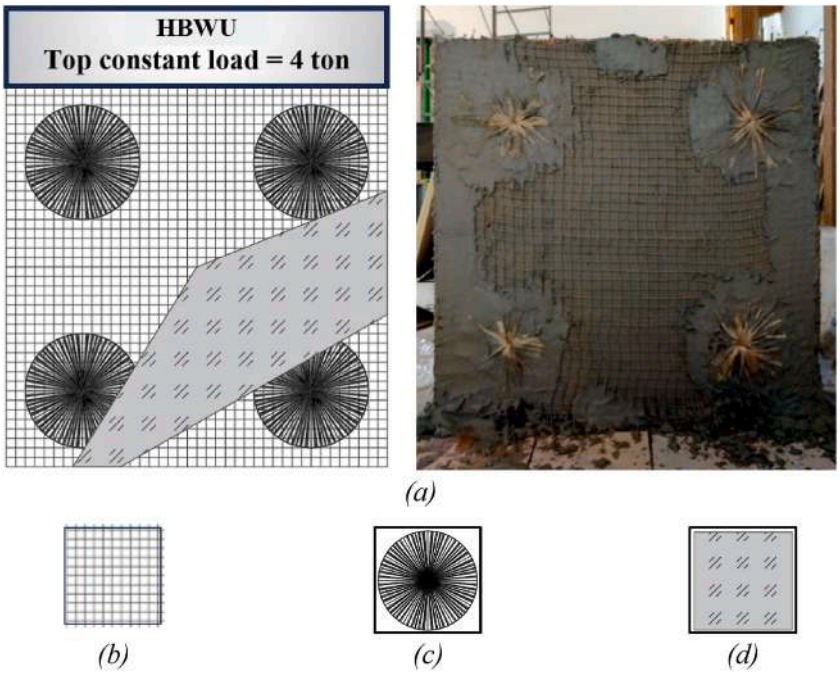

Fig. 10. (a) Masonry walls reinforced with (a) jute net mesh: 2.5 cm × 2.5 cm, (b) 4 jute diatons and (d) jute composite SM with 30 mm jute fiber (1 % with respect to the mortar mass).

Table 6
Various jute fiber derived products used for Masonry wall upgrade.

Samples used	Masonry wall nomenclatures	Dimensions	Mortar used	Composite mortar	Net Type	Mesh type	Number of nets	Number of Diatons	NFTRM layer dimension (each side)
Reference (without upgrade)	HBW 1	1 x 1 × 0.250 m^3	SM	No	No	No	No	No	No NFTRM
Reference (without upgrade)	HBW 2	1 x 1 × 0.250 m^3	SM	No	No	No	No	No	No NFTRM
Structural properties	HBWU	1 x 1 × 0.285 m^3	SM	SM + 1 % jute fiber (30 mm) with respect to mortar mass	1m x 1m	2.5 cm x 2.5 cm	2 (1 on each side)	4	4 cm
Thermal Properties	HBWU(T)	0.7 x 0.9 × 0.285 m^3	SM	SM + 1 % jute fiber (30 mm) with respect to mortar mass	0.9m x 0.7m	2.5 cm x 2.5 cm	2 (1 on each side)	4	4 cm

Note: (1) Jute fiber nets have been used for structural upgrading, (2) Jute fiber diatons are used for structural upgrading, and (3) Whereas jute fiber composite mortar has been used for mainly thermal upgrading, but also help in structural strengthening.

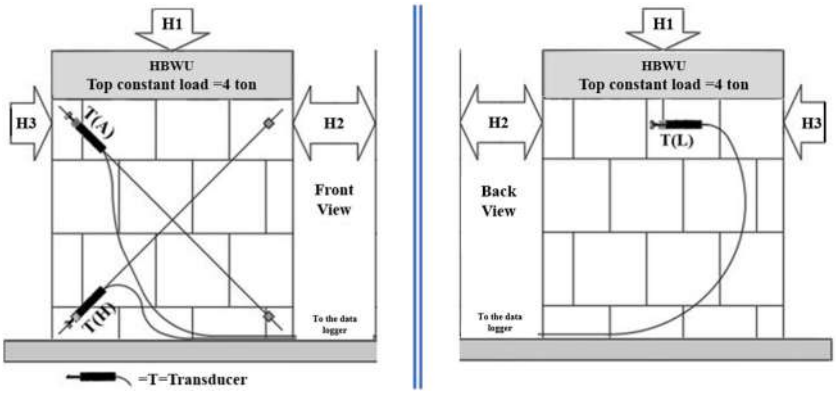

Fig. 11. Masonry wall HBWU: hydraulic jacks and displacements transducers scheme.

Fig. 12. (a) Masonry wall Vs. Upgraded masonry wall (b) HBWU front view, and (c) HBWU back view.

resistance of each layer, therefore, to calculate the overall thermal transmittance of the wall sample (please see section 2.10). The sample HBWU(T) is bit smaller with respect to the HBWU, due to availability of smaller window space inside the central wall of the Climate Chamber (please see section 2.10 to know more), where the tests have been performed.

The retrofitted/upgraded masonry wall HBWU has been subjected to a vertical constant load of 40 kN, see Fig. 10a, Figs. 11 and 12. The not upgraded walls, labelled HBW1 and HBW2, were subjected to vertical loads of 40 kN and 80 kN, respectively. These vertical loads were chosen to represent a small percentage, ranging from 5 % to 10 %, of the ultimate axial capacity of the walls. Subsequently, all the walls underwent an in-plane cyclic test. The quasi-static load protocol is defined as following: at first the vertical load was imposed. Then increasing in-plane cyclic horizontal loads were applied using three horizontal hydraulic jacks. First, the jack H2 gets activated and thereafter the H3, see Fig. 11. At the end of the load cycles, the capacity of the wall is measured using H2 or H3 hydraulic jack with a final load cycle that yields to, the wall collapse. Table 7 and Fig. 12 present the transducers which were used for measuring the diagonal and horizontal displacements. Their nominal displacement is 100 mm, nominal sensitivity 2 mV/V, sensitivity tolerance ±0.1 %, measure resolution 1 μm.

2.9. Thermal conductivity analysis

TAURUS TCA 300 is a heat flow meter, which has been used for Thermal Conductivity (TC) measurements, following ISO 8301 [67] and EN 1946-3 [68]. For TC evaluation a total of four NFTRM samples with upper and lower surface areas equal to 16 × 14 cm^2 "have been used (Fig. 13a). Each sample has a thickness of 4 cm. This obtained TC value (average) has been used for thermal transmittance calculation.

The measuring chamber of the TAURUS has two plates: (1) fixed hot plate, and (2) one mobile cold plate (Fig. 13b). Both upper and lower plates have a surface area of 30 x 30 cm^2. Each plate's main measuring zone is located at the center of the main plates, these active measuring zones have a surface area equal to 10 x 10 cm^2. A heat flux sensor is located at these active zones, and the area surrounding it is the protective zone.

Samples were placed between plates touching upper and lower active zones. Around the sample, a protective insulation woolen panel was placed, in order to minimize/reduce heat losses along the sample's edges and at the same time to have uniform heat flux passing through the sample.

Table 7
Name of Transducers (T), used for measurement for the retrofitted/upgraded masonry wall HBW.

Diagonal displacement Transducers (T)	1. T(A) 2. T(H)
Horizontal displacement Transducers (T)	1. T(L)

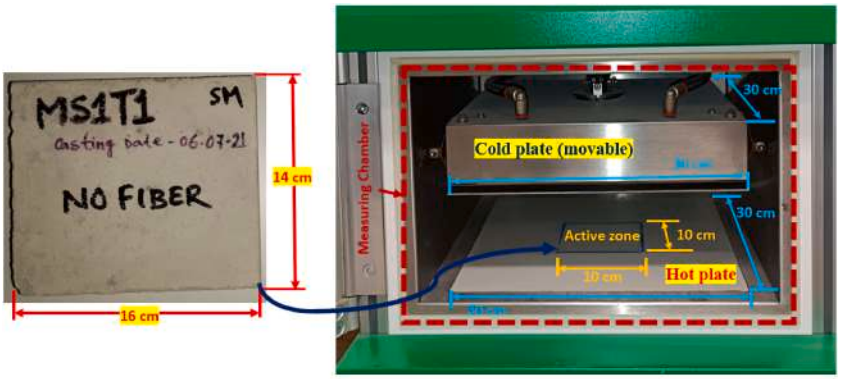

Fig. 13. (a) SM sample "MS1T1" without fiber and (b) TAURUS TCA 300, measuring chamber configuration.

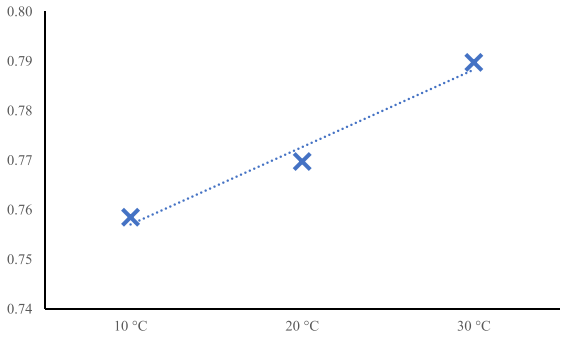

Fig. 14. TC values at different samples mean temperatures, provided by TAURUS TCA 300.

The heat flux instrument was set with an intermediate sampling time of 1 min and a total measuring time of 300 min. According to EN 12939 [69], the mean temperatures of the sample were chosen to be equal to 10 °C, 20 °C and 30 °C. Whereas, the temperature difference between plates was chosen equal to 15 K. The heat fluxes were measured, and the TC value was calculated following Eq (1) [59].

$$\lambda = \dot{Q}\frac{S}{A(t_H - t_C)}\ (\mathrm{W/mK}) \tag{1}$$

where $\dot{Q}$ is the heat flux in (W/m^2), S is the sample thickness in (m), t_H is the hot plate temperature in °C; t_C is the cold plate temperature in °C and A is the active zone surface area of the sample under test.

Fig. 14 presents the TC values provided by the instrument at three set mean temperatures.

2.10. Masonry wall upgrading schemes thermal characterization

Fig. 15 presents the Biemme TH Climate Chamber (CC), located at the University of Cagliari. The CC is designed according to the European regulation [70]. The CC has three parts: two mobile parts (Fig. 15a) and a central fixed (Fig. 15b) wall. Two NFTRM retrofitted/upgraded masonry walls have been constructed inside the central fixed wall of the CC.

These masonry wall HBWU(T) has been retrofitted/upgraded with configuration as shown in Fig. 16 and reported in Table 6. The following steps have been followed while preparing the masonry wall: (a) first of all four holes were drilled, (b) diatons were put

Fig. 15. Climate chamber: (a) main chambers and (b) central wall.

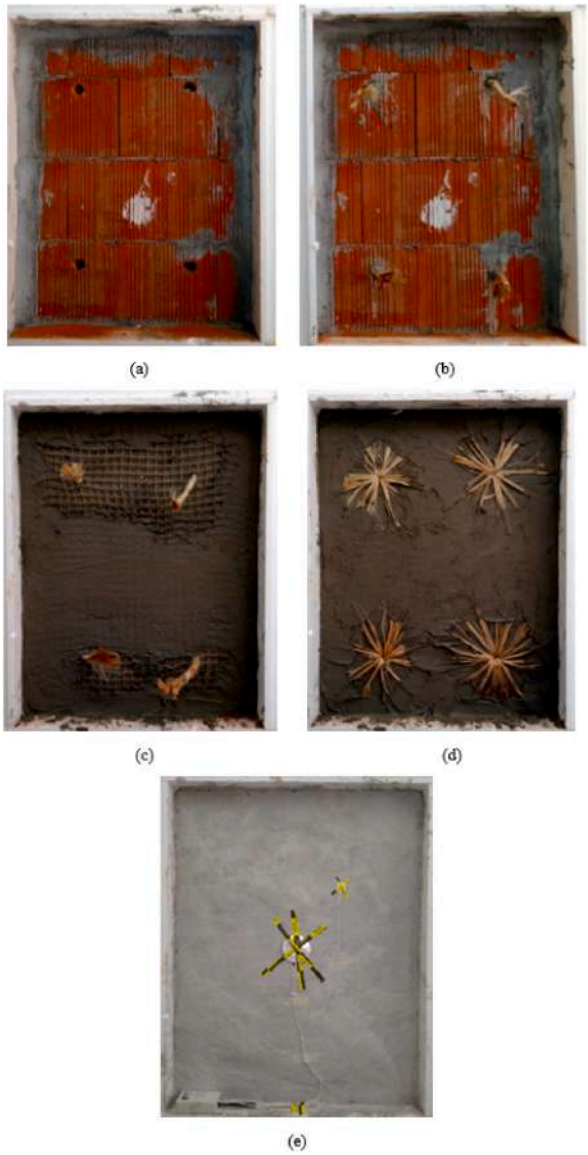

Fig. 16. Masonry wall HBWU(T) upgrade with jute nets, jute diatons and jute fiber composite mortar (SM).

through these holes, (c) a thin layer of mortar has been applied on the walls to attach the jute fiber nets on the walls, (d) the diatons are opened and the upper composite SM layer has been applied (Table 6), Fig. 16 (e) shows the final retrofitted/upgraded masonry wall.

2.11. Thermal conductance measurement

Two different environmental and desired thermodynamic conditions were set for the two chambers (Table 8), and the thermal conductance measurement of the composite walls (0.9 m × 0.7 m) was conducted using CC.

In order to evaluate the thermal conductance of the NFTRM retrofitted/upgraded wall specimens, 2 surface platinum temperature sensors (of class A) and 1 heat flux meter (with accuracy not better than 5 % @T = 20 °C) have been placed on both sides of each specimen (Fig. 17). In addition, the heat flux sensors are also equipped with one temperature sensor incorporated inside them. Parameters like, temperatures (°C), humidity (RH%), and wind velocity (m/s) were measured every 5 min. A wireless system (with the ISM band of 2.4 GHz) and a specific data logger with an integrated RAM have been used for collecting and saving data.

For the aforementioned steady-state conditions test, heat fluxes (W/m^2) and internal and external temperatures (°C) were measured. It has been observed that the quasi-static conditions were attained around after twenty days. The values were generally considered steady when the cumulative moving average value of the heat flux (see Fig. 18) is maintained within the range of ±1 %, at least for consecutive 24 h. Also, in Fig. 18 the daily changes in the internal (room) and the external (ambient) temperatures are presented.

2.12. Thermal transmittance calculation: masonry wall without and with upgrade

Fig. 19 represents the dissection scheme of the NFTRM retrofitted/upgraded masonry wall HBWU(T) with all the layers. The thermal conductance tests were conducted in three steps: (i) for masonry wall without any reinforcement, (ii) masonry wall retrofitted with jute nets, diatons, and SM plaster, and (iii) masonry wall upgraded with jute fiber composite SM.

The thermal resistance labels of the various layers of the retrofitted/upgraded masonry wall are listed in Table 9.

The heat transfers from indoor conditions (with temperature ($T_{in.}$)) to outdoor ambient conditions (with temperature ($T_{Amb.}$)) can be calculated using Eq. (2).

$$\dot{Q} = U \bullet A \bullet \Delta T \,(\mathrm{W}) \tag{2}$$

where,

U is the thermal transmittance (W/m^{2}K), A is the surface area (m^2) and $\Delta T = T_{Amb.} - T_{in}$ (K):

While U can be written as:

$$U = \frac{1}{R_{total}} \,(\mathrm{W}/\mathrm{m}^2\mathrm{K}) \tag{3}$$

where,

R_{Total} being the total thermal resistance in m^{2}K/W.

3. Experimental results

3.1. Structural characterization of the NFTRM upgraded masonry wall HBWU: In-plane cyclic shear test

Masonry sample HBWU has been retrofitted/upgraded with a NFTRM system package (see section 2.6). A constant vertical load of 40 kN has been applied on this wall while three horizontal load cycles were applied to the HBWU wall sample. The first, second and third load cycles are represented with the green curve, the red curve and the black curve, respectively.

Figs. 20 and 21 represent the load-displacement relationship of the diagonal displacement transducer T(A), and diagonal displacement transducer T(H), respectively. While the load-displacement relationship based on the horizontal displacement transducers labelled T(L) is presented in Fig. 22. Depending on the applied force direction the displacements can be negative or positive. The structural behavior of the wall has not been symmetric as can be seen, and a different structural behavior has been recorded when the load is applied from left to right or vice versa.

In the ultimate load cycle, the walls are subjected to a rising horizontal load till the shear collapse that is denoted by an inclined crack starting from the jack application point till the opposite fixed corner of the wall.

The ultimate shear capacities of the not-upgraded (HBW1 and HBW2) and upgraded (HBWU) walls are represented in Fig. 23 that

Table 8
Pre-set desired two environmental conditions.

External ambient conditions (Cold side)			Internal room conditions (Hot side)		
Temperature	Humidity	Ventilation	Temperature	Humidity	Ventilation
(C°)	(RH%)	(m/s)	(C°)	(RH%)	(m/s)
2	50	10.1	20	50	1.1

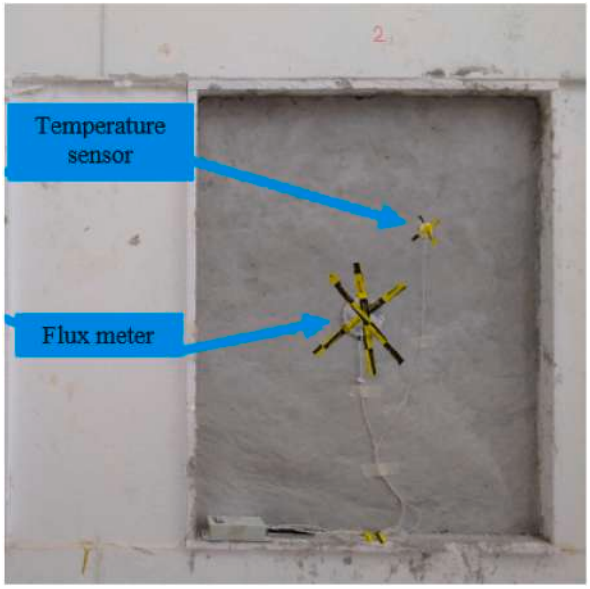

Fig. 17. Masonry wall retrofitting with jute diatons, jute net, and jute fiber structural-composite-mortar.

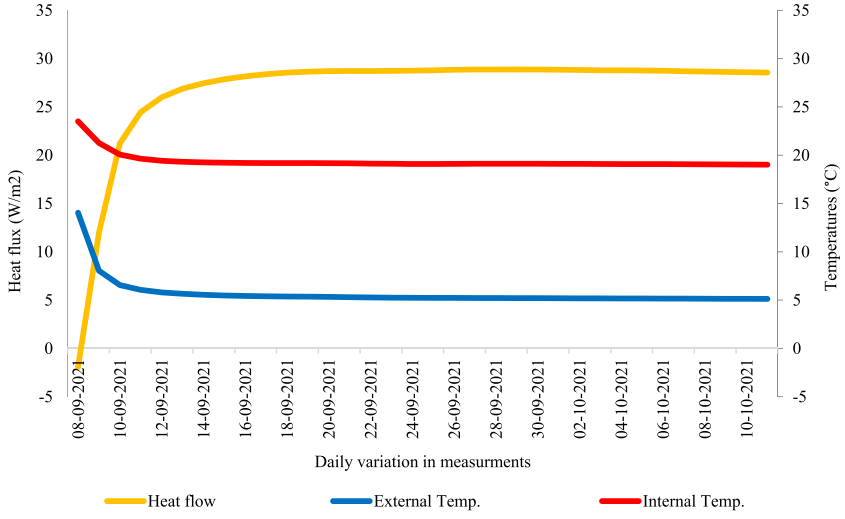

Fig. 18. Change in daily heat flow, external and internal wall surface temperatures measured.

presents the horizontal load-displacements relationships. It is important to remember that the constant vertical loads respectively are 40 kN for HBW1, 80 kN for HBW2 and 40 kN for HBWU. It can be seen that the structural improvement of the TRM system is huge because HBWU a maximum horizontal load that is 4 times the maximum horizontal load of the not upgraded HBW1 and HBW2 walls. In addition, the maximum displacement of HBWU is larger than the ones of HBW1 and HBW2.

Fig. 24 presents the crack pattern which has overserved on the masonry walls HBWU, and it has been highlighted with yellow color. Whereas inside the crack, it can be seen clearly in Fig. 25, the broken net and imbodied jute fibers.

3.2. Theoretical ultimate strengths of the upgraded masonry walls

As established by CNR-DT 215/2018 [14], $V_{t,R}$, the shear capacity of the strengthened wall, could be calculated if the minimum shear capacity of the unreinforced masonry wall, V_t and the contribution of the NFTRM, $V_{t,f}$ are known. $V_{t,R}$ can determined by summing V_t and $V_{t,f}$.

$$V_{t,R} = V_t + V_{t,f} \text{ [kN]} \tag{4}$$

The mechanical parameter "V_t" can be calculated by considering the results of the experimental tests carried out on the reference

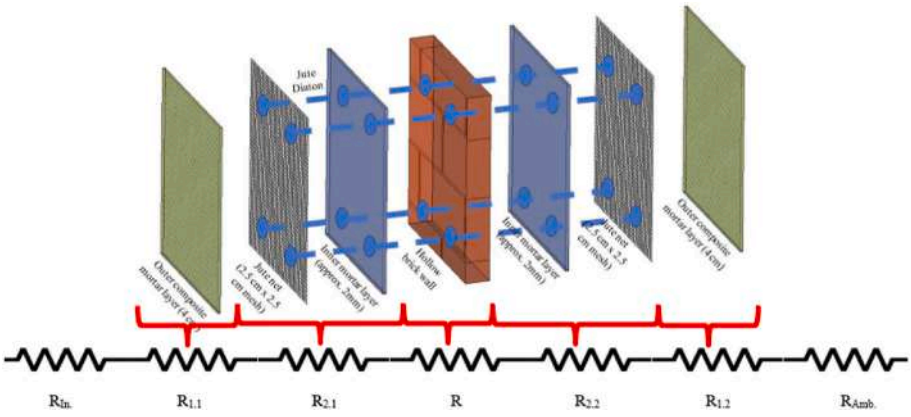

Fig. 19. Thermal resistance for upgraded masonry wall.

Table 9
Layer composition and respective thermal resistance labels of the upgraded masonry wall.

Labels	Indoor resistance
R_{in}	Indoor resistance
$R_{1.1}$	Composite mortar (towards indoor condition) resistance
$R_{2.1}$	Net + diatons + mortar (towards indoor condition) resistance
R_{HB}	Hollow brick resistance
$R_{2.2}$	Net + diatons + mortar (towards outdoor condition) resistance
$R_{1.2}$	Composite mortar (towards outdoor condition) resistance
R_{Amb}	Ambient/outdoor resistance

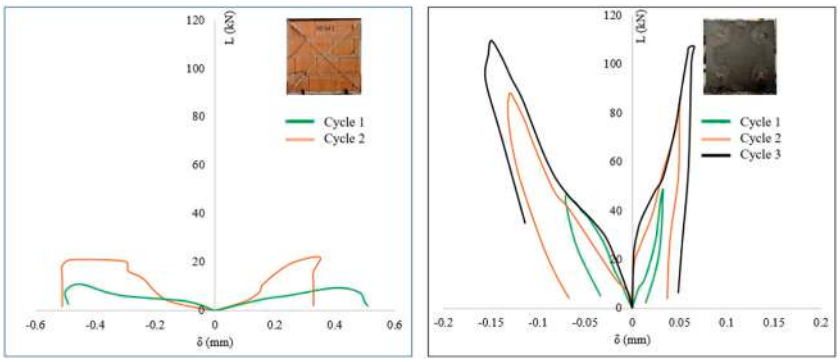

Fig. 20. Load-displacement diagrams: Unreinforced (HBW1) Vs. reinforced (HBWU) masonry wall (when the diagonal sensor A used).

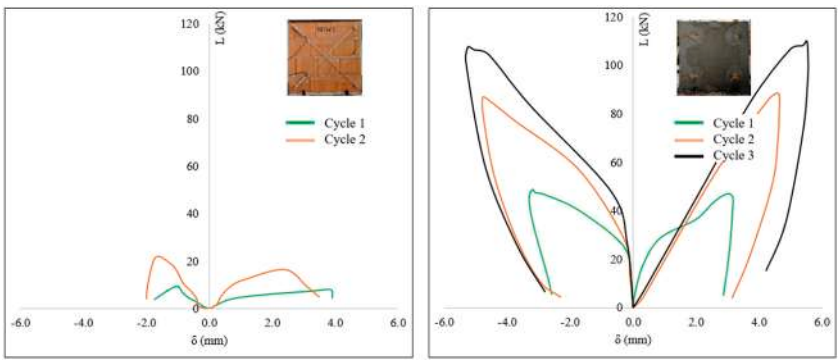

Fig. 21. Load-displacement diagrams: Unreinforced (HBW1) Vs. reinforced (HBWU) masonry walls (when the diagonal sensor H used).

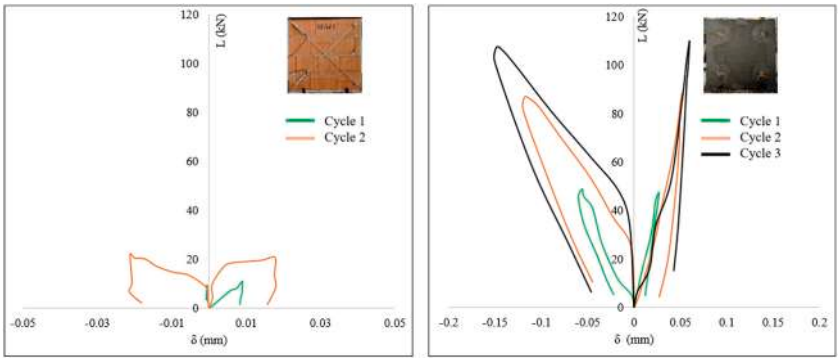

Fig. 22. Load-displacement diagrams: Unreinforced (HBW1) Vs. reinforced (HBWU) masonry walls (when the horizontal sensor L used).

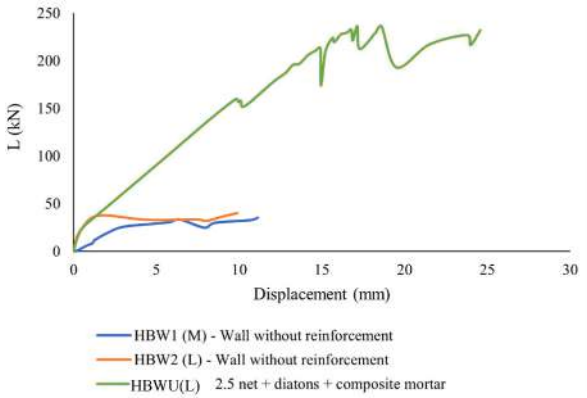

Fig. 23. Ultimate Load cycle.

Fig. 24. HBWU crack pattern after collapse.

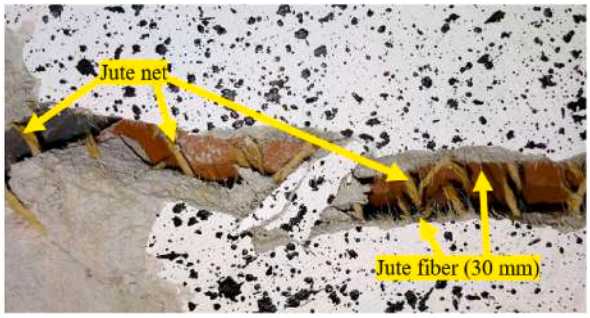

Fig. 25. Composite structure (masonry wall-HBW).

(un-strengthened) specimens. According to the Italian Building Code [62], Vt can be calculated using Eq. (5):

$$V_t = H \cdot t \cdot \frac{1.5\ \tau_{0d}}{p} \sqrt{\left(1 + \frac{\sigma_0}{1.5\ \tau_{0d}}\right)}\ [\text{kN}] \tag{5}$$

where *(H)* is the length, *(l)is the* height and *(t) is* thickness of the masonry wall. During this research campaign un-strengthened masonry walls of dimensions equal to 1000 mm, 1000 mm and 200 mm have been used.

p is a correction coefficient of the stresses in the cross section, its value has been assumed equal to 1.5 as suggested in Ref. [62].

Whereas τ_{0d} (MPa), the reference shear stress capacity can be calculated using Eq. (5) and it has been assumed that V_t equal to the measured experimental value "$V_{t\ exp}$" (Table 10). Therefore, based on this assumption the share stress capacities of the un-strengthened masonry walls have been calculated (Table 10).

σ_0(MPa), the average normal stress, has been calculated (see Table 10) using the following Eq. (6):

$$\sigma_0 = \frac{F_{top}}{H \cdot t}\left[\frac{N}{mm^2}\right] \tag{6}$$

"F_{top}" the stress due to vertical load (it is a fixed load) has been selected/chosen, as reported in Table 10.

The τ_{0d} (MPa) values (see Table 10) of both un-strengthened masonry walls interestingly found to be in the range in-between 0.10 – 0.13 [MPa], the value available according to Italian NTC18 [71] for the semi-hollow brick wall (i.e., Masonry with semi-solid clay bricks, with dry vertical joints (holes percentage <45 %)).

Therefore, the overall contribution of the masonry wall V_t was re-calculated using Eq. (3), for this calculation average of the two parameters i.e., τ_{od} and σ_0 has been done and the value obtained is equal to 38.01 [kN].

The contribution of the NFTRM system $V_{t,f}$ has been calculated following the Italian Building Code [62] using Eq. (7):

$$V_{t,f} = \frac{1}{\gamma_{Rd}} . n_f . t_{vf} . l_f . \alpha_t . \varepsilon_{fd} . E_f\ [\text{kN}] \tag{7}$$

where γ_{Rd} is the partial safety factor, here it has been considered equal to 1.

n_f is the total number of the reinforced layers arranged at each side of the wall, here n_f is equal to 1.

t_{vf} is the equivalent thickness of a single layer of the NFTRM system and it is equal to 4 cm in our case.

l_f is the design dimension of the reinforcement measured orthogonally to the shear force, it can't be longer than the length of the masonry wall. Therefore $l_f \leq H$. Here it is equal to 1000 mm for all the specimens.

α_t is the coefficient to account for the reduced tensile strength of fibers when under shear stress. According to Ref. [14] this value is assumed equal to 0.80.

E_f is the Young's/elastic modulus of elasticity of dry fabric/textile,

ε_{fd} is the design strain of NFTRM.

Table 10
Set, measured, and calculated in-plane cyclic load test values of the normal (un-upgraded) masonry walls.

	Set fixed top load (set value)	Experimental maximum horizontal force (measured value)	Average normal stress (calculated value)	Shear stress capacity (calculated value)
	F_{top}	$V_{t\ exp}$	σ_0	τ_{0d}
	[kN]	[kN]	[MPa]	[MPa]
HBW1(80 kN)	79.68	40.00	0.3984	0.1073
HBW2(40 kN)	39.84	35.41	0.1992	0.1227

So, the design strength of the NFTRM system is:

$$\sigma_{fd} = \varepsilon_{fd}.\, E_f \text{ [MPa]} \tag{8}$$

Therefore, Eq. (5) can be re-written as:

$$V_{t,f} = \frac{1}{\gamma_{Rd}}.n_f.t_{vf}.l_f.\alpha_t.\sigma_{fd} \text{ [kN]} \tag{9}$$

The shear capacity of the strengthened wall, $V_{t,R}$ should be equal to the measured experimental value of the maximum horizontal force (see Table 8).

The contribution of the NFTRM system, i.e., $V_{t,f}$ should be equal to:

$$V_{t,f} = V_{t,R} - V_t \text{ [kN]} \tag{10}$$

The value "$V_{t.\ exp.}$" of the un-strengthened masonry wall is experimentally evaluated (see Table 10). In addition, the experimental value of the maximum horizontal force ($V_{t,R\ .\ exp.}$) withstand by the upgraded masonry wall has been measured and it found to be equal to 236,21 [kN] (Table 11).

Here it is important to highlight that the un-strengthened masonry wall was upgraded with a total number of "2" NFTRM system packages (jute nets, jute diatons and jute fiber composite SM with 1 % fiber (30 mm) with respect to the mortar mass), applied one on each side of the masonry wall.

Therefore, Eq. (10) can be modified and the TOTAL contribution of "2" NFTRM system can be calculated (see Table 11) as below:

$$V_{t,f.TOTAL} = V_{t,R\ .\ exp.} - V_{t.\ exp.} \text{[kN]} \tag{11}$$

Further it has been considered that both NFTRM system package contributes equally to enhance overall strength, therefore the load bearing capacity of the upgraded masonry wall.

Now the contribution of a single NFTRM system package can be calculated as (see Table 11):

$$V_{t,f} = \frac{V_{t,f.TOTAL}}{2} \text{[kN]} \tag{12}$$

Actually, if $\varepsilon_{u,f}$ denotes the ultimate strain of the NFTRM system, therefore its ultimate strength is equal to:

$$\sigma_{u,f} = \varepsilon_{u,f}.\, E_f \text{ [MPa]} \tag{13}$$

To assess the ultimate limit state capacity of the NFTRM we enforce Eq. (13) into Eq. (9). Indeed, here, we consider that the ultimate strength $\sigma_{u,f}$ equal to the design strength σ_{fd}. Thus, the contribution of the NFTRM system can be equal to:

$$V_{t,f} = \frac{1}{\gamma_{Rd}}.n_f.t_{vf}.l_f.\alpha_t.\sigma_{u,f} \text{ [kN]} \tag{14}$$

Therefore, the ultimate strength of the NFTRM system has been calculated using:

$$\sigma_{u,f} = \frac{V_{t,f}}{\frac{1}{\gamma_{Rd}}.n_f.t_{vf}.l_f.\alpha_t} = \frac{V_{t,R} - V_t}{\frac{1}{\gamma_{Rd}}.n_f.t_{vf}.l_f.\alpha_t} \text{ [MPa]} \tag{15}$$

Using Eq. (15) the ultimate strength of a single NFTRM system package (jute nets, jute diatons and jute fiber composite SM with 1 % fiber (30 mm) with respect to the mortar mass) can be calculated and it is found to be equal to 3.097 MPa.

Notably, the overall contribution of the NFTRM system packages is very significant, considering the structural upgrading of the un-reinforced masonry wall. Interestingly, a single NFTRM system package can enhance 2.6 times additional strength, when compared to the strength of the un-strengthen masonry wall.

3.3. Thermal characterization of the NFTRM masonry wall thermal conductance tests

The composite wall HBWU(T) was constructed inside the Climatic Chamber's (CC) central wall. HBWU(T) was built layer by layer, similar as shown in Fig. 16.

Measured heat flow (W/m^2), indoor temperature (°C) and outdoor temperatures (°C) data [72] have been used for the thermal

Table 11
The ultimate strengths of the TRM system of the tested masonry walls.

Upgraded masonry wall	Net Mesh gap	Equivalent thickness of a single layer of the NFTRM system	Maximum Experimental horizontal force (Measured)	Total NFTRM contribution (Calculated using Eq. (10))	Contribution of a single NFTRM system package (Calculated using Eq. (11))
		t_{vf}	$V_{t,R.exp}$	$V_{t,f.TOTAL}$	$V_{t,f.}$
	[mm]	[mm]	[kN]	[kN]	[kN]
HBWU (40 kN)	25.0	40.00	236.21	198.20	99,10

Table 12
Thermal resistance of each tested layer of the composite masonry wall system.

Mortar type	R_{in} (Indoor) UNI EN 6946:2018 [72]	$R_{1.1}$ (Composite mortar)	$R_{2.1}$ (Net + Diatons + mortar)	R_{HB} (Hollow brick wall)	$R_{2.2}$ (Net + Diatons + mortar)	$R_{1.2}$ (Composite mortar)	R_{Amb} (Ambient) UNI EN 6946:2018 [72]
	m^2K/W	m^2K/W	m^2K/W	m^2K/W	m^2K/W	m^2K/W	m^2K/W
Thickness SM	0.040	20 mm 0.0440	2 mm 0.1149	0.3935	2 mm 0.1149	20 mm 0.0440	0.130

resistance (m^2K/W) calculated for each layer, and reported in Table 12.

Eq. (16) [73] has been used for the total thermal resistance $R_{Total.1}$ (m^2K/W) calculation for the composite wall NFTRM system package, see Table 12 for the meaning of each symbol.

$$R_{Total.1} = R_{In.} + R_{1.1} + R_{2.1} + R_{HB} + R_{2.2} + R_{1.2} + R_{Amb.} \left[m^2K / W\right] \tag{16}$$

Additionally, another upgrading configuration was also considered: the masonry wall with just SM plaster (see Fig. 26). Thus, the thermal transmittance of the masonry wall with only SM plaster layer (U_2) was calculated and compared with the composite wall system retrofitted/upgraded with the NFTRM system package.

The thermal resistance (R_{SM}) of the SM layer is calculated according to Eq. (17). If the plaster is applied to the masonry wall (0.9 m $\times$ 0.7 m) surfaces and it has thickness (S) of approximately 2 mm, the thermal conductivity (λ) value of the SM (without fiber) is equal to 0.77 W/mK.

$$R_{SM} = \frac{S}{A \bullet \lambda} \left(m^2K / W\right) \tag{17}$$

If the SM plaster is applied on both sides of the masonry wall, the total thermal resistance (m^2K/W) using Kirchhoff current law can be written using Eq. (18), where R_{In} is the indoor thermal resistance, $R_{1.SM}$ and $R_{2.SM}$ are the thermal resistances of the SM plaster layer and $R_{Amb.}$ Is the outdoor/ambient thermal resistance.

$$R_{Total.2} = R_{In.} + R_{1.SM} + R_{HB} + R_{2.SM} + R_{Amb.} \left(m^2K / W\right) \tag{18}$$

The measured, calculated and reference thermal resistance values of different layers of the masonry wall with SM only are summarized in Table 13.

The inverse of the thermal resistance is defined as thermal transmittance U. The latter values for the normal un-strengthened

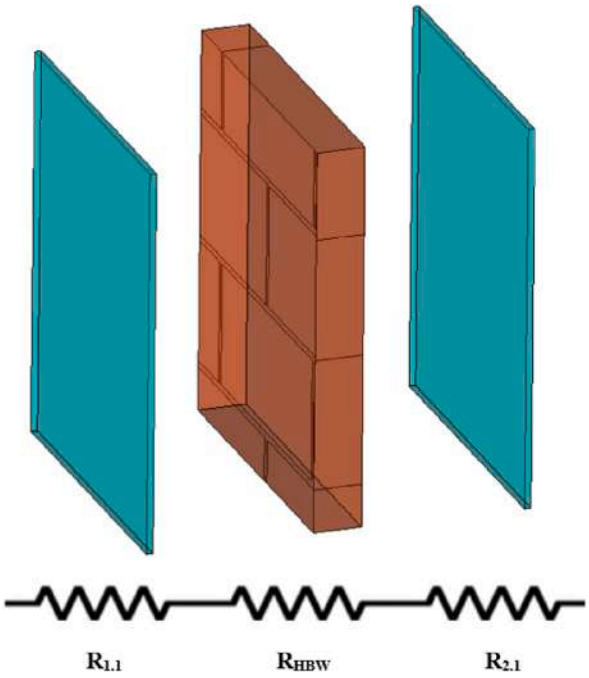

Fig. 26. Thermal resistance of a masonry wall with SM plaster layers.

Table 13
Thermal resistance of each layer of the masonry wall with SM applied on surfaces.

Masonry wall reinforcement mortar type	R_{in} (Indoor) UNI EN 6946:2018 [72]	$R_{1.SM}$ (Structural mortar layer)	R_{HB} (Hollow brick wall)	$R_{2.SM}$ (Structural mortar layer)	R_{Amb} (Ambient) UNI EN 6946:2018 [72]
	m^2K/W	m^2K/W	m^2K/W	m^2K/W	m^2K/W
Thickness		2 mm		2 mm	
SM	0.040	0.0039	0.3935	0.0039	0.1300

Table 14
Thermal transmittance: Hollow brick masonry wall Vs Hollow brick reinforced composite wall system.

U_1 Masonry wall	U_2 Masonry wall + SM plaster	U_3 Upgraded masonry wall: Masonry wall + jute net + jute diatons + SM Plaster + Jute fiber composite mortar
W/m^2K	W/m^2K	W/m^2K
1.770	1.748	1.135

masonry wall (U_1), for the masonry wall with 2 mm SM plaster (U_2) and for the composite wall retrofitted/upgraded with NFTRM system package (i.e., masonry walls upgraded with jute fiber products i.e. jute net, jute diatons and jute fiber composite mortar) U_3, are respectively evaluated and can be found in Table 14.

Therefore, it is clear that, with the application of only SM plaster on the masonry wall yields a very little reduction in the thermal transmittance value, which is around 0.022 W/m^2K, the composite wall yields a reduction in the thermal transmittance value of about 0.635 W/m^2K.

3.4. Discussion on the integrated behavior of the upgraded masonry wall

The wall specimen type HBWU has been considered to evaluate the integrated (structural and thermal behaviors) performance of the NFTRM system package which has been used for retrofitting/upgrading the masonry wall.

The HBWU has been upgraded with jute nets (with mesh 2.5 cm × 2.5 cm), jute fiber diatons and composite SM (prepared with 1 % fiber (30 mm) with respect to the dry mortar mass).

The jute nets and jute diatons mainly have been used for structural strengthening, while the outer composite layers have been used particularly for thermal upgrade i.e., to enhance the insulation capacity of the masonry wall. But it has been observed that this composite SM too has helped in enhancing the retrofitted/upgraded masonry wall's strength.

Due to the application of the NFTRM system package (Fig. 27), the improvement in overall withstanding horizontal load capacity increased by more than 520 %, and the thermal transmittance value reduced by around - 35.00 % when compared with masonry wall without any upgrade.

Table 15 provides a crucial comparative analysis between innovative natural fiber Textile Reinforced Mortar (TRM) systems and traditional man-made fiber TRM systems, highlighting both structural and thermal retrofitting/upgrading results. This comparison is significant as it showcases the emerging potential of natural fibers like jute in applications traditionally dominated by synthetic

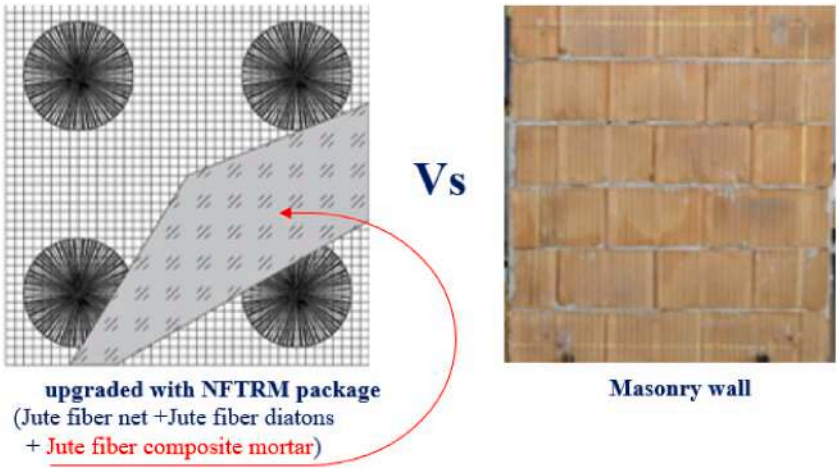

Fig. 27. Upgraded masonry wall (HBWU) compared with un-strengthened masonry wall.

Table 15
Observation/findings and comparison between Integrated natural fiber TRM system Vs. Man-made fiber TRM system.

	Material used for structural retrofitting/ upgrading	Structural property (min., max. or avg. values)	Material used for thermal retrofitting/upgrading	Insulation property (IP) (min., max. or avg. values)
In this current project: Natural fiber (jute fiber) Integrated (structural and thermal) retrofitting/upgrading.				
Masonry wall upgraded with NFTRM (Natural Fiber TRM)	Jute fiber net, Jute fiber diatons, jute fiber composite mortar TRM	In-plane cyclic tests: Maximum horizontal load Reference wall (experimental) 35.21 (kN) Vs. Upgraded masonry wall (experimental) 236.21 (kN). Ultimate strength of NFTRM system and contribution (experimental) 198.20 (kN).	Jute fiber composite mortar prepared with 1 % of jute fiber (30 mm) with respect to the dry mortar.	Obtained thermal transmittance obtained for: Reference wall (experimental) 1.770 (W/m^2K) Vs. all retrofitting/upgrading wall samples (experimental) 1.135 (W/m^2K)
Reference research works: Integrated (structural and thermal) retrofitting/upgrading.				
Triantafillou, T.C. et al. (2017) [49]	Commercially available man-made fiber TRM	Three-point bending tests: Peak loads Reference wall (experimental) 3.42 (kN) Vs. all retrofitting/upgrading wall samples (experimental) 8.06 (kN) – 20.26 (kN);	EPS	Improvement in IP is considered due to the application of EPS.
Triantafillou, T.C. et al. (2018) [50]	Glass fiber TRM	Three-point bending tests: Peak loads Reference wall (experimental) 19.9 (kN) for type-A, 20 (kN) for type-B, and 12.2 (kN) for type-C Vs. Considering all retrofitting/ upgrading wall samples (experimental) 31.5 (kN) - 37.5 (kN) for Type-A, 29.2–37.1 (kN) for type-B and 24.3 (kN) – 36.8 (kN) for type-C, respectively.	EPS	Improvement in IP is considered due to the application of EPS.
Gkournelos, P.D. et al. (2020) [51]	Commercially available man-made fiber TRM	In-plane tests: Shear strength - Reference wall (experimental) 0.78 (MPa) Vs. Integrated wall (experimental) 1.63 (MPa). Out-of-plane tests: Maximum average load – Reference wall (experimental) 1.60 (kN) Vs. Integrated wall (experimental average with and without pre-in-plane failure) 25.3 (kN)	EPS	Improvement in IP is considered due to the application of EPS.
Karlos, K. et al. (2020) [52]	Glass fiber TRM	Three-point bending tests: Peak loads Reference wall (experimental) 3.42 (kN) Vs. Peak loads (experimental) 9.28 (kN) – 20.26 (kN);	EPS	Improvement in IP is considered due to the application of EPS.
Facconi, L. et al. (2021) [53]	Steel fiber TRM	Full scale building test. Horizontal peak force reference wall 180 (kN) Vs Horizontal peak force retrofitted wall 605 (kN)	Aerogel, light wood fiber, and heavy wood fiber.	Obtained thermal transmittance obtained for: Reference wall (analytical) 1.038 (W/m^2K) Vs. all retrofitting/upgrading wall samples (analytical) 0.242 (W/m^2K) – 0.335 (W/m^2K) and all retrofitting/upgrading wall samples (numerical) 0.246 (W/m^2K) – 0.336 (W/m^2K)
Longo, F. et al. (2021) [54]	AR dry glass, Glass and steel fiber TRM	Obtained Shear strength for glass fibers retrofitting/upgrading: 0.818 (MPa) – 1.298 (MPa). Obtained Shear strength for steel fibers retrofitting/upgrading: 1.058 (MPa) – 1.480 (MPa).	Hydraulic lime and GeoPolymer lime	Obtained thermal transmittance obtained for Reference wall (experimental) 2.082 (W/m^2K) Vs. all retrofitting/upgrading wall samples (experimental) 1.051 (W/m^2K) – 1.562 (W/m^2K)

(*continued on next page*)

Table 15 (*continued*)

	Material used for structural retrofitting/ upgrading	Structural property (min., max. or avg. values)	Material used for thermal retrofitting/upgrading	Insulation property (IP) (min., max. or avg. values)
Baek, E. et al. (2022) [55]	Basalt fabric TRM	Lateral load capacity (average): Reference wall (experimental) – 52.7 (kN) Vs. Textile capillary tube panel (TCP) reinforced masonry wall – 74.55 (kN) and TCP-TRM reinforced masonry wall – 119.15 (kN)	Textile capillary tube panel (TCP) layer: hot water was channeled through the tube to obtain the desired room temperature.	Improvement in masonry wall IP has been observed by using the TCP system the room temperature was maintained at around 20 °C. Better performance has been observed when the TCP layer has been placed internally.
Gkournelos, P.D. et al. (2023) [56]	Commercially available man-made fiber TRM	In-plane tests: Shear strength - Reference wall (experimental) near-about 140 (kN) Vs. Integrated wall (experimental) near-about 160 (kN). Out-of-plane tests: Maximum peak load – Reference wall (experimental average with and without pre-in-plane failure) 47.4 (kN) Vs. Integrated wall (experimental average with and without pre-in-plane failure) 69.2 (kN)	EPS	Improvement in IP is considered due to the application of EPS.
Furtado, A. et al. (2023) [57]	Glass fiber TRM	Out-of-plane tests: Maximum peak load – Reference wall near-about 45 (kN) Vs. considering all retrofitting/ upgrading wall samples (experimental) in between 65 (kN) – 100 (kN)	EPS, ETICS (external thermal insulation composite system) and Reinforced Thermal Insulation Mortar (RTIM)	Obtained thermal transmittance obtained for: Reference wall (calculated) near-about 1.75 (W/m^2K) Vs. considering all retrofitting/ upgrading wall samples (calculated) in between 0.30 (W/m^2K) – 0.4 (W/m^2K).

materials, such as glass fibers, basalt, and polymeric substances like EPS.

The use of jute fibers in NFTRM packages demonstrated a substantial increase in the structural capacity of masonry walls, showing a remarkable improvement in maximum horizontal load-bearing from 35.21 kN in reference walls to 236.21 kN in upgraded walls. This underscores the strength and viability of jute fiber TRM systems in structural applications. In contrast, traditional man-made fibers have been primarily valued for their high tensile strength and durability. However, the performance metrics across different studies, as cited in the literature, vary significantly depending on the fiber type and matrix compatibility.

The innovative use of jute fiber composite mortar significantly reduced the thermal transmittance from 1.770 W/m^2K in reference walls to 1.135 W/m^2K. This improvement in thermal insulation capabilities is competitive with enhancements observed with synthetic TRM systems, where materials like EPS and ETICS are commonly employed due to their lower thermal transmittance but often at the cost of structural integrity.

Man-made fibers such as glass and basalt, are generally associated with higher costs and environmental impact in production, compared to natural fibers like jute, which are sustainable, less energy-intensive to produce, and offer significant environmental benefits, including biodegradability.

Each type of fiber material offers distinct advantages depending on the specific application requirements. Man-made fibers perform exceptionally well in environments requiring high durability and minimal degradation over time. Natural fibers, while relatively new in this application, show promise not only in mechanical performance but also in sustainability, making them ideal for projects with an environmental focus.

As the construction industry moves towards more sustainable practices, the integration of natural fibers into retrofitting projects could play a pivotal role in reducing the ecological footprint of construction materials. Continued research and development into the treatment and processing of natural fibers will enhance their durability, potentially matching or even surpassing the performance of synthetic fibers in certain aspects.

This study represents the first instance of employing natural fiber (jute fiber) products for simultaneous structural and thermal integrated retrofitting/upgrading. The structural and thermal properties were systematically evaluated through in-plane structural tests and thermal conductivity measurements conducted within a controlled climate chamber.

Table 15 not only illustrates the current state of research into fiber-reinforced masonry wall retrofitting, but also highlights the need for a broader understanding of material properties and their long-term behavior. This understanding will guide the construction industry towards making informed choices about material sustainability, cost-effectiveness, and overall structural and thermal

performance. Through detailed comparisons and empirical data, we can better appreciate the nuances of each material type, leading to more innovative and ecologically responsible building practices.

4. Conclusions

This paper reported on a comprehensive approach to the integrated structural and thermal upgrading of masonry walls, employing jute fiber-derived products in a Natural Fiber Textile Reinforced Mortar (NFTRM) system. The innovative NFTRM system, which includes jute nets, jute fiber diatons, and a jute fiber composite mortar, offers significant improvements in both the mechanical and thermal performance of masonry walls.

From the in-plane cyclic shear tests, it was observed that the NFTRM system contributed to an 8.4 % increase in ultimate strength when compared to un-strengthened walls, demonstrating its structural efficacy. Furthermore, the application of the jute-based composite mortar enhanced the thermal insulation of the retrofitted walls, resulting in a 36 % reduction in thermal transmittance compared to non-upgraded masonry walls.

These findings underscore the dual functionality of the jute NFTRM system, which not only provides substantial improvements in load-bearing capacity—by as much as 520%—but also effectively reduces heat transfer, thereby aligning with modern energy efficiency standards. This integrated upgrading approach, which leverages sustainable natural fibers, contributes to the broader goals of energy-efficient building retrofitting while minimizing environmental impact.

Future research is necessary to optimize the NFTRM system by determining the most effective thickness and configuration of jute fiber layers to further refine the balance between structural reinforcement and thermal insulation. Moreover, while the jute diatons' potential contribution to thermal resistance was not fully explored in this study, it will be a focus of subsequent investigations to fully quantify their impact.

In addition, while this study highlights the structural and thermal benefits of using jute fiber products for masonry wall upgrades, the long-term durability of these materials, especially under varied environmental conditions, remains an open issue. Future research should focus on extensive durability assessments of jute fiber and its products to ensure that they meet the long-term service-life requirements of brick masonry structures. This would involve evaluating the effects of moisture, temperature fluctuations, and biological factors on the longevity and performance of jute fibers, thus aligning with sustainable building practices and ensuring reliability of these materials over extended periods.

In conclusion, the use of jute-based NFTRM systems presents a promising, eco-friendly solution for the integrated upgrading of masonry buildings, addressing both seismic safety and energy efficiency concerns in a single intervention.

CRediT authorship contribution statement

Flavio Stochino: Writing – original draft, Validation, Supervision, Methodology, Investigation, Data curation, Conceptualization. **Arnas Majumder:** Writing – original draft, Methodology, Investigation, Data curation. **Andrea Frattolillo:** Writing – review & editing, Resources, Methodology, Formal analysis, Conceptualization. **Monica Valdes:** Writing – review & editing, Methodology, Investigation, Data curation. **Enzo Martinelli:** Writing – review & editing, Project administration, Funding acquisition, Conceptualization.

Declaration of competing interest

The authors declare no conflict of interest for the manuscript entitled "Jute Fiber Reinforcement for Masonry Walls: Integrating Structural Strength and Thermal Insulation in Sustainable Upgrades"

Acknowledgement

The financial support of the PRIN PNRR 2022 - project Integra TRM: Integrated seismic and thermal upgrading of existing masonry buildings through a novel sustainable Textile-Reinforced Mortar system F53D23009850001 is acknowledged.

Data availability

Data will be made available on request.

References

[1] C. European, Boosting the renovation rate of existing masonry buildings in earthquake-prone EU regions, seismic plus EneRgy upgrading of masonry buildings using advanced materials, Horizon 2020 (2020). https://cordis.europa.eu/article/id/430350-boosting-the-renovation-rate-of-existing-masonry-buildings-in-earthquake-prone-eu-regions. (Accessed 26 March 2024).

[2] A. Majumder, F. Stochino, F. Fraternali, E. Martinelli, Seismic and thermal retrofitting of masonry buildings with fiber reinforced composite systems: a state of the art review, Int. J. Struct. Glass Adv. Mater. Res. 5 (2021) 41–67, https://doi.org/10.3844/sgamrsp.2021.41.67.

[3] E. Martinelli, F. Perri, C. Sguazzo, C. Faella, Cyclic shear-compression tests on masonry walls strengthened with alternative configurations of CFRP strips, Bull. Earthq. Eng. 14 (2016) 1695–1720, https://doi.org/10.1007/s10518-016-9895-6.

[4] EN 1998-3, Eurocode 8, Design of Structures for Earthquake Resistance – Part 3: Assessment and Retrofitting of Buildings, 2005.

[5] N. Longarini, P. Crespi, M. Zucca, The influence of the geometrical features on the seismic response of historical churches reinforced by different cross lam roof-solutions, Bull. Earthq. Eng. 20 (2022) 6813–6852, https://doi.org/10.1007/s10518-022-01468-y.

[6] A. Franchi, P. Napoli, P. Crespi, N. Giordano, M. Zucca, Unloading and Reloading Process for the Earthquake Damage Repair of Ancient Masonry Columns: The Case of the Basilica di Collemaggio, Int. J. Architect. Herit. 16 (2022) 1683–1698, https://doi.org/10.1080/15583058.2021.1904056.

[7] M. Zucca, P.G. Crespi, N. Longarini, M.A. Scamardo, The new foundation system of the Basilica di Collemaggio's transept, IJMRI 5 (2020) 67, https://doi.org/10.1504/IJMRI.2020.104846.

[8] European Commission. Joint Research Centre, Building Stock Inventory to Assess Seismic Vulnerability across Europe, Publications Office, LU, 2018. https://data.europa.eu/doi/10.2760/530683. (Accessed 26 March 2024).

[9] E. Commission, Energy efficiency in buildings, European. https://commission.europa.eu/news/focus-energy-efficiency-buildings-2020-02-17_en, 2020. (Accessed 16 March 2024).

[10] Buildings, (n.d.). https://www.iea.org/energy-system/buildings (accessed March 26, 2024).

[11] EN 1998-1, Eurocode 8, design of structures for earthquake rsistance. Part 1: General Rules, Seismic Actions and Rules for Buildings, 2004.

[12] EN ISO 52016-1, Energy Performance of Buildings and Building Components, 2017.

[13] EU 2018/844, Directive (EU) 2018/844 of the European Parliament and of the Council of 30 May 2018 amending Directive 2010/31/EU on the energy performance of buildings and Directive 2012/27/EU on energy efficiency. https://eur-lex.europa.eu/legal-content/EN/TXT/?uri=uriserv:OJ.L_.2018.156.01.0075.01.ENG, 2018. (Accessed 26 March 2024).

[14] CNR-DT 215/2018, Guide for the design and construction of externally bonded fibre reinforced inorganic matrix systems for strengthening existing structures. https://www.cnr.it/en/node/12827, 2019. (Accessed 26 March 2024).

[15] G. Ferrara, C. Caggegi, E. Martinelli, A. Gabor, Shear capacity of masonry walls externally strengthened using Flax-TRM composite systems: experimental tests and comparative assessment, Constr. Build. Mater. 261 (2020) 120490, https://doi.org/10.1016/j.conbuildmat.2020.120490.

[16] L. Estevan, B. Torres, F.J. Baeza, F.B. Varona, S. Ivorra, Masonry walls strengthened with Textile Reinforced Mortars (TRM) and subjected to in-plane cyclic loads after real fire exposure, Eng. Struct. 296 (2023) 116922, https://doi.org/10.1016/j.engstruct.2023.116922.

[17] S. De Santis, G. De Canio, G. De Felice, P. Meriggi, I. Roselli, Out-of-plane seismic retrofitting of masonry walls with Textile Reinforced Mortar composites, Bull. Earthq. Eng. 17 (2019) 6265–6300, https://doi.org/10.1007/s10518-019-00701-5.

[18] RILEM Technical Committee 232-TDT (Wolfgang Brameshuber), Recommendation of RILEM TC 232-TDT: test methods and design of textile reinforced concrete: uniaxial tensile test: test method to determine the load bearing behavior of tensile specimens made of textile reinforced concrete, Mater. Struct. 49 (2016) 4923–4927, https://doi.org/10.1617/s11527-016-0839-z.

[19] American Concrete Institute, in: Guide to Design and Construction of Externally Bonded Fabric-Reinforced Cementitious Matrix (FRCM) Systems for Repair and Strengthening Concrete and Masonry Structures, American Concrete Institute, Farmington Hills, Mich, 2013.

[20] M.T. De Risi, A. Furtado, H. Rodrigues, J. Melo, G.M. Verderame, A. Arêde, H. Varum, G. Manfredi, Influence of textile reinforced mortars strengthening on the in-plane/out-of-plane response of masonry infill walls in RC frames, Eng. Struct. 254 (2022) 113887, https://doi.org/10.1016/j.engstruct.2022.113887.

[21] H.H. Pham, N.H. Dinh, S.-H. Kim, S.-H. Park, K.-K. Choi, Tensile behavioral characteristics of lightweight carbon textile-reinforced cementitious composites, J. Build. Eng. 57 (2022) 104848, https://doi.org/10.1016/j.jobe.2022.104848.

[22] A. Prota, G. Marcari, G. Fabbrocino, G. Manfredi, C. Aldea, Experimental in-plane behavior of tuff masonry strengthened with cementitious matrix–grid composites, J. Compos. Construct. 10 (2006) 223–233, https://doi.org/10.1061/(ASCE)1090-0268(2006)10:3.223.

[23] C. Faella, E. Martinelli, E. Nigro, S. Paciello, Shear capacity of masonry walls externally strengthened by a cement-based composite material: an experimental campaign, Constr. Build. Mater. 24 (2010) 84–93, https://doi.org/10.1016/j.conbuildmat.2009.08.019.

[24] L. Guo, M. Deng, R. Li, T. Li, Z. Dong, Shear strengthening of RC short columns with CFRP grid-reinforced FRC matrix: cyclic loading tests, J. Build. Eng. 47 (2022) 103915, https://doi.org/10.1016/j.jobe.2021.103915.

[25] S. Li, X. Chen, Z. Liu, Y. Lu, H. Wang, Axial behavior of pre-damaged RC columns strengthened with CFRP textile grid-reinforced ECC matrix composites, J. Build. Eng. 73 (2023) 106813, https://doi.org/10.1016/j.jobe.2023.106813.

[26] A. Furtado, H. Rodrigues, A. Arêde, Cantilever flexural strength tests of masonry infill walls strengthened with textile-reinforced mortar, J. Build. Eng. 33 (2021) 101611, https://doi.org/10.1016/j.jobe.2020.101611.

[27] N. Gattesco, I. Boem, E. Rizzi, A. Dudine, M. Gams, Cyclic tests on two-leaf rubble stone masonry spandrels strengthened with CRM coating on one or both sides, Eng. Struct. 296 (2023) 116965, https://doi.org/10.1016/j.engstruct.2023.116965.

[28] F. Akhoundi, G. Vasconcelos, P. Lourenço, In-plane behavior of infills using glass fiber shear connectors in textile reinforced mortar (TRM) technique, Int. J. Struct. Glass Adv. Mater. Res. 2 (2018) 1–14, https://doi.org/10.3844/sgamrsp.2018.1.14.

[29] A.C.H. Giese, D.N. Giese, V.F.P. Dutra, L.C.P. Da Silva Filho, Flexural behavior of reinforced concrete beams strengthened with textile reinforced mortar, J. Build. Eng. 33 (2021) 101873, https://doi.org/10.1016/j.jobe.2020.101873.

[30] J. Wang, C. Wan, L. Shen, Q. Zeng, X. Ji, Compressive behavior of masonry columns confined with basalt textile-reinforced concrete, J. Build. Eng. 75 (2023) 107019, https://doi.org/10.1016/j.jobe.2023.107019.

[31] M. Ibrahim, M. Galal, M. Kohail, A. Rashad, H. ElShafie, Behaviour of unreinforced masonry walls retrofitted by using basalt textile reinforced mortar, Eng. Struct. 260 (2022) 114201, https://doi.org/10.1016/j.engstruct.2022.114201.

[32] L. Pérez-Pinedo, C. Sandoval, R. Alvarado, L. Vargas, S. Calderón, E. Bernat, Seismic strengthening of partially grouted masonry walls with openings: evaluation of ferrocement and BTRM solutions, J. Build. Eng. 88 (2024) 109235, https://doi.org/10.1016/j.jobe.2024.109235.

[33] A.R. Kamrava, M.A. Najafgholipour, F. Fathi, S.M. Dehghan, An experimental study on the in-plane behavior of unreinforced masonry walls with an opening strengthened using steel fiber reinforced concrete overlays, J. Build. Eng. 36 (2021) 102084, https://doi.org/10.1016/j.jobe.2020.102084.

[34] M. Fossetti, G. Minafò, Strengthening of masonry columns with BFRCM or with steel wires: an experimental study, Fibers 4 (2016) 15, https://doi.org/10.3390/fib4020015.

[35] L. Facconi, S.S. Lucchini, F. Minelli, G.A. Plizzari, Analytical model for the in-plane resistance of masonry walls retrofitted with steel fiber reinforced mortar coating, Eng. Struct. 275 (2023) 115232, https://doi.org/10.1016/j.engstruct.2022.115232.

[36] M.T. Ferrandez-García, C.E. Ferrandez-Garcia, T. Garcia-Ortuño, A. Ferrandez-Garcia, M. Ferrandez-Villena, Study of waste jute fibre panels (Corchorus capsularis L.) agglomerated with portland cement and starch, Polymers 12 (2020) 599, https://doi.org/10.3390/polym12030599.

[37] J.M. Ferreira, C. Capela, J. Manaia, J.D. Costa, Mechanical properties of woven mat jute/epoxy composites, Mater. Res. 19 (2016) 702–710, https://doi.org/10.1590/1980-5373-MR-2015-0422.

[38] A. Formisano, G. Chiumiento, E.J. Dessì, Laboratory tests on hydraulic lime mortar reinforced with jute fibres, TOCIEJ 14 (2020) 152–162, https://doi.org/10.2174/1874149502014010152.

[39] A. Majumder, F. Stochino, A. Frattolillo, M. Valdes, F. Fraternali, E. Martinelli, Sustainable building material: recycled jute fiber composite mortar for thermal and structural retrofitting, in: O. Gervasi, B. Murgante, S. Misra, A.M.A.C. Rocha, C. Garau (Eds.), Computational Science and its Applications – ICCSA 2022 Workshops, Springer International Publishing, Cham, 2022, pp. 657–669, https://doi.org/10.1007/978-3-031-10545-6_44.

[40] A. Majumder, M. Achenza, C.C. Mastino, R. Baccoli, A. Frattolillo, Thermo-acoustic building insulation materials fabricated with recycled fibers – jute, Wool and Loofah, Energy Build. 293 (2023) 113211, https://doi.org/10.1016/j.enbuild.2023.113211.

[41] A. Majumder, F. Stochino, A. Frattolillo, M. Valdes, F. Fraternali, E. Martinelli, Jute fiber mortar composites for integrated retrofitting, in: 14th Fib PhD Symposium in Civil Engineering, the International Federation for Structural Concrete, 2022, pp. 613–620. Rome.

[42] A. Majumder, I. Farina, F. Stochino, F. Fraternali, E. Martinelli, Natural fibers reinforced mortars: composition and mechanical properties, KEM 913 (2022) 149–153, https://doi.org/10.4028/p-027t71.

[43] A. Majumder, L. Canale, C.C. Mastino, A. Pacitto, A. Frattolillo, M. Dell'Isola, Thermal characterization of recycled materials for building insulation, Energies 14 (2021) 3564, https://doi.org/10.3390/en14123564.

[44] A. Razmi, M.M. Mirsayar, On the mixed mode I/II fracture properties of jute fiber-reinforced concrete, Constr. Build. Mater. 148 (2017) 512–520, https://doi.org/10.1016/j.conbuildmat.2017.05.034.
[45] M.A. Saleem, S. Abbas, M. Haider, Jute fiber reinforced compressed earth bricks (FR-CEB)–a sustainable solution., Pakistan J. Eng. Appl. Sci. (n.d.). https://www.bing.com/ck/a?!&&p=a01f5dc4b4f25143JmltdHM9MTcxMTQxMTIwMCZpZ3VpZD0xM2ZmNzg5OS0zYjc0LTYyNTAtMGQ1NS02YjdkM2EzMTYzZGEmaW5zaWQ9NTI0Mw&ptn=3&ver=2&hsh=3&fclid=13ff7899-3b74-6250-0d55-6b7d3a3163da&psq=%5b37%5d+Saleem%2c+M.A.%2c+Abbas%2c+S.+and+Haider%2c+M.%2c+2016.+Jute+fiber+reinforced+compressed+earth+bricks+(FR-CEB)%e2%80%93a+sustainable+solution.+Pakistan+Journal+of+Engineering+and+Applied+Sciences.&u=a1aHR0cHM6Ly9qb3VybmFsLnVldC5lZHUucGsvb2pzX29sZC9pbmRleC5waHAvcGplYXMvYXJ0aWNsZS9kb3dubG9hZC8yODUvMjIz&ntb=1 (accessed March 26, 2024).
[46] C. Menna, D. Asprone, M. Durante, A. Zinno, A. Balsamo, A. Prota, Structural behaviour of masonry panels strengthened with an innovative hemp fibre composite grid, Constr. Build. Mater. 100 (2015) 111–121, https://doi.org/10.1016/j.conbuildmat.2015.09.051.
[47] N. Trochoutsou, M. Di Benedetti, K. Pilakoutas, M. Guadagnini, Mechanical characterisation of flax and jute textile-reinforced mortars, Constr. Build. Mater. 271 (2021) 121564, https://doi.org/10.1016/j.conbuildmat.2020.121564.
[48] E. Baek, D.A. Pohoryles, S. Kallioras, D.A. Bournas, H. Choi, T. Kim, Innovative seismic and energy retrofitting of wall envelopes using prefabricated textile-reinforced concrete panels with an embedded capillary tube system, Eng. Struct. 265 (2022) 114453, https://doi.org/10.1016/j.engstruct.2022.114453.
[49] T.C. Triantafillou, K. Karlos, K. Kefalou, E. Argyropoulou, An innovative structural and energy retrofitting system for URM walls using textile reinforced mortars combined with thermal insulation: mechanical and fire behavior, Constr. Build. Mater. 133 (2017) 1–13, https://doi.org/10.1016/j.conbuildmat.2016.12.032.
[50] T.C. Triantafillou, K. Karlos, P. Kapsalis, L. Georgiou, Innovative structural and energy retrofitting system for masonry walls using textile reinforced mortars combined with thermal insulation: in-plane mechanical behavior, J. Compos. Construct. 22 (2018) 04018029, https://doi.org/10.1061/(ASCE)CC.1943-5614.0000869.
[51] P.D. Gkournelos, T.C. Triantafillou, D.A. Bournas, Integrated structural and energy retrofitting of masonry walls: effect of in-plane damage on the out-of-plane response, J. Compos. Construct. 24 (2020) 04020049, https://doi.org/10.1061/(ASCE)CC.1943-5614.0001066.
[52] K. Karlos, A. Tsantilis, T. Triantafillou, Integrated seismic and energy retrofitting system for masonry walls using textile-reinforced mortars combined with thermal insulation: experimental, analytical, and numerical study, J. Compos. Sci. 4 (2020) 189, https://doi.org/10.3390/jcs4040189.
[53] L. Facconi, S.S. Lucchini, F. Minelli, B. Grassi, M. Pilotelli, G.A. Plizzari, Innovative method for seismic and energy retrofitting of masonry buildings, Sustainability 13 (2021) 6350, https://doi.org/10.3390/su13116350.
[54] F. Longo, A. Cascardi, P. Lassandro, M.A. Aiello, Energy and seismic drawbacks of masonry: a unified retrofitting solution, J. Build. Rehabil. 6 (2021) 31, https://doi.org/10.1007/s41024-021-00121-6.
[55] E. Baek, D.A. Pohoryles, S. Kallioras, D.A. Bournas, H. Choi, T. Kim, Innovative seismic and energy retrofitting of wall envelopes using prefabricated textile-reinforced concrete panels with an embedded capillary tube system, Eng. Struct. 265 (2022) 114453, https://doi.org/10.1016/j.engstruct.2022.114453.
[56] P.D. Gkournelos, T.C. Triantafillou, Out-of-Plane behavior of in-plane damaged masonry infills retrofitted with TRM and thermal insulation, J. Compos. Construct. 27 (2023) 04023054, https://doi.org/10.1061/JCCOF2.CCENG-4324.
[57] A. Furtado, H. Rodrigues, A. Arêde, H. Varum, A experimental characterization of seismic plus thermal energy retrofitting techniques for masonry infill walls, J. Build. Eng. 75 (2023) 106854, https://doi.org/10.1016/j.jobe.2023.106854.
[58] A. Majumder, F. Stochino, I. Farina, M. Valdes, F. Fraternali, E. Martinelli, Physical and mechanical characteristics of raw jute fibers, threads and diatons, Constr. Build. Mater. 326 (2022) 126903, https://doi.org/10.1016/j.conbuildmat.2022.126903.
[59] A. Majumder, F. Stochino, A. Frattolillo, M. Valdes, G. Mancusi, E. Martinelli, Jute fiber-reinforced mortars: mechanical response and thermal performance, J. Build. Eng. 66 (2023) 105888, https://doi.org/10.1016/j.jobe.2023.105888.
[60] A. Majumder, F. Stochino, A. Frattolillo, M. Valdes, G. Gatto, E. Martinelli, Sustainable retrofitting solutions: evaluating the performance of jute fiber nets and composite mortar in natural fiber textile reinforced mortars, Sustainability 16 (2024) 1175, https://doi.org/10.3390/su16031175.
[61] NTC18, NTC18 Italian building code 'Norme Tecniche per le Costruzioni ' Ministero delle infrastrutture e dei Trasporti, in Italian., (n.d.).
[62] NTC18, NTC18 Application Circular of NTC18, Circolare n. 7 del 21 Gennaio 2019,"Istruzioni per l'applicazione dell'«Aggiornamento delle "Norme tecniche per le costruzioni", in Italian (2019) n.d.
[63] UNI EN 998-2:2010, Specification for Plastering and Rendering: External Renders, 2010.
[64] EN 1015-2:2007, Methods of Test for Mortar for Masonry—Part 2: Bulk Sampling of Mortars and Preparation of Test Mortars, 2007.
[65] EN 13501-1, Fire Classification of Products and Building Elements - Part1: Classification Using Data from Reaction to Fire Tests, European Committee for Standardization, 2019.
[66] Poroton Italia, Semi-solid blocks P800. https://www.poroton.it/mattoni-laterizi/blocchi-semipieni-p800/, 2024 (accessed March 4, 2024).
[67] ISO 8301:1991, Thermal Insulation, Determination of Steady-State Thermal Resistance and Related Properties—Heat Flow Meter Apparatus, International Organization for Standardization, 1991.
[68] EN 1946-3, Thermal Performance of Building Products and Components — Specific Criteria for the Assessment of Laboratories Measuring Heat Transfer Properties — Part 3: Measurements by the Heat Flow Meter Method, European Committee for Standardization, 1999.
[69] EN 12939, Thermal Performance of Building Materials and Products—Determination of Thermal Resistance by Means of the Hot Plate with Guard Ring and the Heat Flow Meter Method—Thick Products with High and Medium Thermal Resistance, European Committee for Standardization, 2002.
[70] UNI EN 1934, Thermal Performance of Buildings - Determination of Thermal Resistance by Hot Box Method Using Heat Flow Meter - Masonry, 2000 n.d.
[71] Application Circular of NTC18, Circolare n. 7 del 21 Gennaio 2019,"Istruzioni per l'applicazione dell'«Aggiornamento delle "Norme tecniche per le costruzioni", in Italian (2019) n.d.
[72] UNI EN ISO 6946, Building Components and Building Elements - Thermal Resistance and Thermal Transmittance - Calculation Methods, 2018 n.d.
[73] H. Nowak, Ł. Nowak, Non-destructive possibilities of thermal performance evaluation of the external walls, Materials 14 (2021) 7438, https://doi.org/10.3390/ma14237438.